

2-1-2012

# An Empirical Method for Correcting the Detector Spectral Response in Energy-Resolved CT

Taly Gilat Schmidt

Marquette University, tal.gilat-schmidt@marquette.edu

---

Published version. Published as part of the proceedings of the conference, *SPIE Medical Imaging*, 2012: DOI. © 2012. Society of Photo-Optical Instrumentation Engineers. One print or electronic copy may be made for personal use only. Systematic reproduction and distribution, duplication of any material in this paper for a fee or for commercial purposes, or modification of the content of the paper are prohibited.

# An empirical method for correcting the detector spectral response in energy-resolved CT

Taly Gilat Schmidt

Department of Biomedical Engineering, Marquette University, Milwaukee, WI, USA;

## ABSTRACT

Energy-resolving photon-counting detectors have the potential for improved material decomposition compared to dual-kVp approaches. However, material decomposition accuracy is limited by the nonideal spectral response of the detectors. This work proposes an empirical method for correcting the nonideal spectral response, including spectrum-tailing effects. Unlike previous correction methods which relied on synchrotron measurements, the proposed method can be performed on the scanner. The proposed method estimates a spectral-response matrix by performing x-ray projection measurements through a range of known thicknesses of two or more calibration materials. Once estimated, the spectral-response matrix is incorporated into conventional material decomposition algorithms. A simulation study investigated preliminary feasibility of the proposed method. The spectral-response matrix was estimated using simulated projection measurements through PMMA, aluminum, and gadolinium. An energy-resolved acquisition of a thorax phantom with gadolinium in the blood pool was simulated assuming a five-bin detector with realistic spectral response. Energy-bin data was decomposed into Compton, photoelectric, and gadolinium basis projections with and without the proposed correction method. Basis images were reconstructed by filtered backprojection. Results demonstrated that the nonideal spectral response reduced the ability to distinguish gadolinium from materials such as bone, while images reconstructed with the proposed correction method successfully depicted the contrast agent. The proposed correction method reduced errors from 9% to 0.6% in the Compton image, 90% to 0.6% in the photoelectric image and from 40% to 6% in the gadolinium image when using a three-material calibration. Overall, results support feasibility of the proposed spectral-response correction method.

**Keywords:** energy-resolved CT, photon counting, calibration

## 1. INTRODUCTION

Material decomposition using multi-energy data has shown promise for numerous clinical applications including kidney stone characterization and vascular imaging. Energy-resolving direct-conversion semiconductor detectors have several potential advantages compared to clinically available dual-kVp methods, including reduced motion sensitivity, higher dose efficiency, and the ability to differentiate multiple k-edge contrast agents.<sup>1</sup> However, several effects in the detection process limit the ability of direct-conversion detectors to measure true photon energy, for example incomplete charge collection, charge-sharing between neighboring pixels, k-fluorescence escape, and pulse-pileup.<sup>2</sup> Assuming the absence of pulse-pileup, the net result of these effects is the detection of high-energy photons in low-energy bins. The nonideal spectral response can introduce error when energy-resolved data is used for material decomposition and optimal energy weighting.<sup>3</sup> Spectral response effects become more severe when pixel size is reduced to prevent pulse-pileup effects.

Previously proposed spectral-response correction methods required knowledge of the complete spectral response.<sup>2,4</sup> In these previous studies, the spectral-response functions were measured through synchrotron measurements or other advanced technology. Another alternative is to measure the spectral response through isotope measurements.

This work proposes an empirical method for correcting the spectral response of energy-resolved detectors. Unlike previous methods, the proposed method uses projection data of a calibration phantom. The performance of the correction method for material decomposition applications is investigated through simulations of a voxelized thorax phantom.

---

Further author information: (Send correspondence to T.G.S.)  
taly.gilat-schmidt@marquette.edu

## 2. METHODS

### 2.1 Proposed Correction Method

The true detector spectral response is continuous in both the incident photon energy and the detected photon energy. The response functions,  $R(E, E')$ , represent the probability of an incident photon at energy  $E'$  being detected at energy  $E$ . These spectral-response functions were previously measured at a synchrotron facility and analytically modeled for a CdTe detector.<sup>2</sup>

To reduce the dimensionality of the unknown spectral response, we propose modeling the spectral response with a  $B \times B$  matrix,  $\mathbf{R}$ , where  $B$  is the number of discrete energy bins in the detector. Each coefficient  $R_{i,j}$  represents the fraction of photons detected in bin  $i$  whose true energy belongs in bin  $j$ .

We propose estimating the spectral-response matrix,  $\mathbf{R}$ , by performing x-ray projection measurements on a range of known thicknesses of two or more calibration materials, for example PMMA and Aluminum, with the beam collimated to reduce scatter. For each detector pixel, the calibration procedure results in  $M$  total measurements for each of the  $B$  bins. The measurements are arranged into a  $B \times M$  matrix,  $\hat{\mathbf{A}}$ . In the absence of noise:

$$\hat{\mathbf{A}} = \mathbf{R}\mathbf{A} \quad (1)$$

where  $\mathbf{A}$  is the matrix containing the  $B \times M$  measurements that would be acquired with an ideal energy response. The ideal measurements,  $A_{i,j}$ , can be predicted based on the known incident spectrum and the known material properties and lengths. For example,

$$A_{i,j} = \int_{E_i} N_o(E) \exp(\mu_j(E)T_j) dE \quad (2)$$

where  $N_o(E)$  is the incident spectrum,  $E_i$  is the energy range of the  $i^{th}$  bin, and  $\mu_j$  and  $T_j$  are the attenuation coefficient and thickness of the  $j^{th}$  slab. In summary,  $\hat{\mathbf{A}}$  is measured,  $\mathbf{A}$  can be modeled based on prior knowledge of the spectrum and calibration materials, and  $\mathbf{R}$  contains the  $B \times B$  unknowns representing the spectral response. The spectrum,  $N_o(E)$ , which is also required for material decomposition, can be estimated from the energy bin that counts all photons above the lowest energy threshold using previously proposed spectrum estimation techniques.<sup>5</sup> Our previous work demonstrated that this bin is primarily unaffected by the nonideal spectral response.<sup>3</sup>

Matrix  $\mathbf{R}$  has known properties that can be used to further constrain the estimation, for example nonnegativity. We can also make the assumption that low-energy photons are not detected in higher-energy bins (i.e.,  $R_{i,j} = 0$  for all  $i > j$ ). At most, all photons must be detected in some bin, therefore the sum along any of the columns of  $\mathbf{R}$  must be less than or equal to one.

$$\sum_{j=1}^B R_{i,j} \leq 1 \quad (3)$$

Once the incident spectrum is estimated, least squares or maximum likelihood methods can estimate  $\mathbf{R}$  using the relationship in Eq. 1.

Material decomposition is performed by finding the basis material path lengths that best match the measured data in each energy bin for each ray. For each ray, the following system of equations is determined:

$$\begin{aligned} n_1 &= \int_{E_1} N_o(E) \exp \left[ - \sum c_k \int \mu_k(E, t) dt \right] dE \\ n_2 &= \int_{E_2} N_o(E) \exp \left[ - \sum c_k \int \mu_k(E, t) dt \right] dE \\ &\dots \\ n_B &= \int_{E_B} N_o(E) \exp \left[ - \sum c_k \int \mu_k(E, t) dt \right] dE \end{aligned} \quad (4)$$

Table 1. Simulated system specifications

Number of detector pixels	700
Pixel size	1 mm
Source-to-isocenter distance	50 cm
Source-to-detector distance	100 cm
Number of views	500
Spectrum	120 kVp, 6 mm Al
mAs	200
Energy-bin ranges	[20-50], [51-59], [60-69], [70-89], [90-120] keV

where  $E_i$  is the energy range of the  $i^{th}$  bin, and  $c_k$  and  $\mu_k$  are respectively the basis coefficient and attenuation coefficient of the  $k^{th}$  basis material.

The vector of energy-bin measurements,  $\hat{\vec{n}}$ , is related to the measurements expected from an ideal detector,  $\vec{n}$  by the following relationship:

$$\hat{\vec{n}} = \mathbf{R}\vec{n} \quad (5)$$

By incorporating Eq. 5 into the forward model of Eq. 4, material decomposition algorithms can estimate the basis line integrals that best match the observed data, including the nonideal spectral response.

## 2.2 Simulation Study

Feasibility of the proposed spectral-response correction method was investigated through simulations. Table 1 lists the specifications of the simulated system. All polyenergetic simulations were performed by modeling monoenergetic x-rays at 20-120 keV in 1 keV increments. The incident spectrum was modeled according to the SPEC78 software.<sup>6</sup> Attenuation coefficients were modeled according to the XCOM database.<sup>7</sup> Poisson noise was added to the simulated ray measurements. To model a realistic spectral response, empirically determined spectral-response functions<sup>2</sup> were modeled as part of the simulation.<sup>3</sup>

The simulated calibration materials were 10 slabs of PMMA (2 to 20 cm) and aluminum (1 to 10 cm). Calibration measurements were simulated with photon noise assuming the specifications listed in Table 1. The spectral-response matrix  $\mathbf{R}$  was estimated from Eq. 1 by maximizing the likelihood of the observed measurements, using a constrained interior point nonlinear minimization algorithm. The initial guess for  $\mathbf{R}$  was the identity matrix (i.e., ideal energy response).

While the true spectral-response functions are object independent, the spectral-response matrix  $\mathbf{R}$  depends on the detected spectrum and thus the object. These object-dependent effects are expected to be small except potentially in the case of K-edge contrast agents. To understand these effects, a second calibration was performed with projections through ten concentrations of gadolinium (gadolinium weight fractions of 0.0193 - 0.0386) added to the calibration measurements.

The correction method was evaluated by simulating a 120 kVp, 200 mAs, five-bin energy-resolved acquisition (Table 1) of a voxelized thorax phantom. The phantom was created by segmenting a CT image into 18 tissue types and varying concentrations of gadolinium in the blood pool, as depicted in Figure 1. The transmission of photons of energy 20-120 keV in 1 keV increments was calculated, with the spectral-response function modeled for each energy. The energy-resolved projections were decomposed into photoelectric, Compton, and Gadolinium basis projections with and without the proposed spectral-response correction using a maximum likelihood estimation method.<sup>1</sup> Basis images were reconstructed by filtered backprojection. The mean value was calculated in regions of interest (ROIs) in the heart muscle, calcification, and blood pool of the reconstructed Compton, photoelectric, and gadolinium basis images, respectively (Figure 2), and compared to values resulting from a detector with ideal energy response.

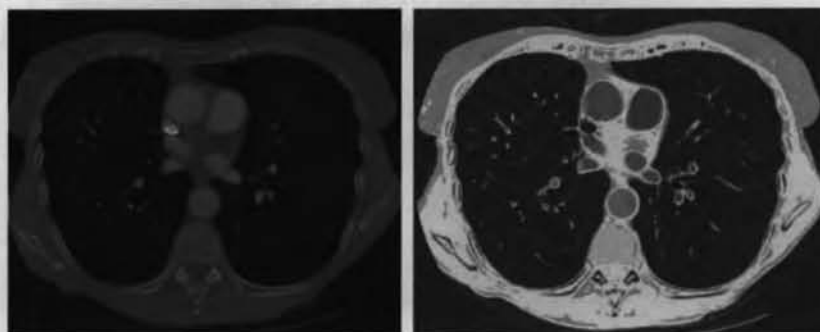


Figure 1. (left) CT image which was segmented to create the (right) resulting thorax phantom.

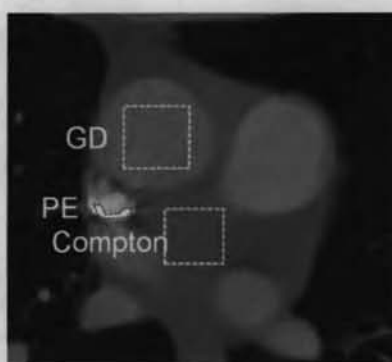


Figure 2. The ROIs extracted from the reconstructed Compton, photoelectric, and gadolinium basis images.

### 3. RESULTS

Figure 3 displays Compton, photoelectric, and gadolinium basis images reconstructed from energy-resolved data modeling ideal and realistic spectral response, with and without the proposed correction method. Spectral response correction was performed using both the two-material (PMMA and Al) and three-material (PMMA, Al, Gd) calibration. Figure 3 demonstrates that the nonideal spectral response reduces the ability to distinguish gadolinium from materials such as bone and causes substantial errors in the photoelectric basis images. Images reconstructed with the proposed correction method successfully depict the contrast agent and photoelectric image. Table 2 compares the percent error measured in ROIs in Compton, photoelectric, and gadolinium basis images resulting from energy-resolved data with realistic spectral response decomposed with and without the proposed correction method.

### 4. DISCUSSION AND CONCLUSIONS

The proposed correction method reduced errors from 9% to 0.6% in the Compton image, 89% to 0.6% in the photoelectric image and from 40% to 6% in the gadolinium image when using a three-material calibration. The

Table 2. Percent error in reconstructed basis images

	Realistic	Two-material correction	Three-material correction
Compton	9%	0.2%	0.6%
Photoelectric	89.4%	5.0%	0.6%
Gadolinium	39.8%	13.7%	5.7%



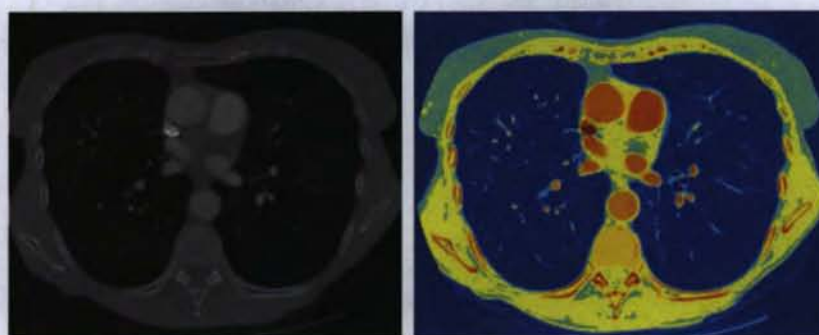


Figure 1. (left) CT image which was segmented to create the (right) resulting thorax phantom.



Figure 2. The ROIs extracted from the reconstructed Compton, photoelectric, and gadolinium basis images.

### 3. RESULTS

Figure 3 displays Compton, photoelectric, and gadolinium basis images reconstructed from energy-resolved data modeling ideal and realistic spectral response, with and without the proposed correction method. Spectral response correction was performed using both the two-material (PMMA and Al) and three-material (PMMA, Al, Gd) calibration. Figure 3 demonstrates that the nonideal spectral response reduces the ability to distinguish gadolinium from materials such as bone and causes substantial errors in the photoelectric basis images. Images reconstructed with the proposed correction method successfully depict the contrast agent and photoelectric image. Table 2 compares the percent error measured in ROIs in Compton, photoelectric, and gadolinium basis images resulting from energy-resolved data with realistic spectral response decomposed with and without the proposed correction method.

### 4. DISCUSSION AND CONCLUSIONS

The proposed correction method reduced errors from 9% to 0.6% in the Compton image, 89% to 0.6% in the photoelectric image and from 40% to 6% in the gadolinium image when using a three-material calibration. The

Table 2. Percent error in reconstructed basis images

	Realistic	Two-material correction	Three-material correction
Compton	9%	0.2%	0.6%
Photoelectric	89.4%	5.0%	0.6%
Gadolinium	39.8%	13.7%	5.7%

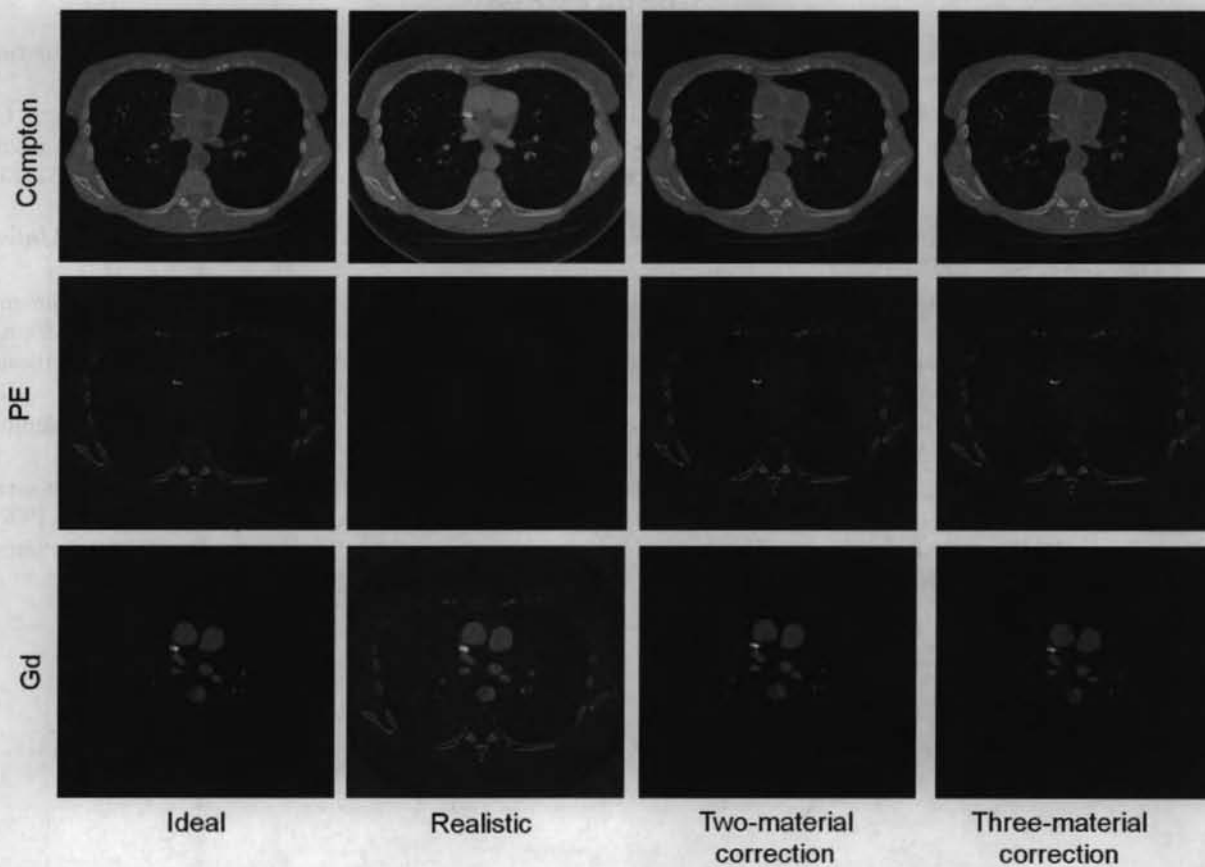


Figure 3. Reconstructed Compton, photoelectric, and gadolinium basis images reconstructed from a detector with an ideal response, realistic spectral response with and without the proposed two and three material correction.



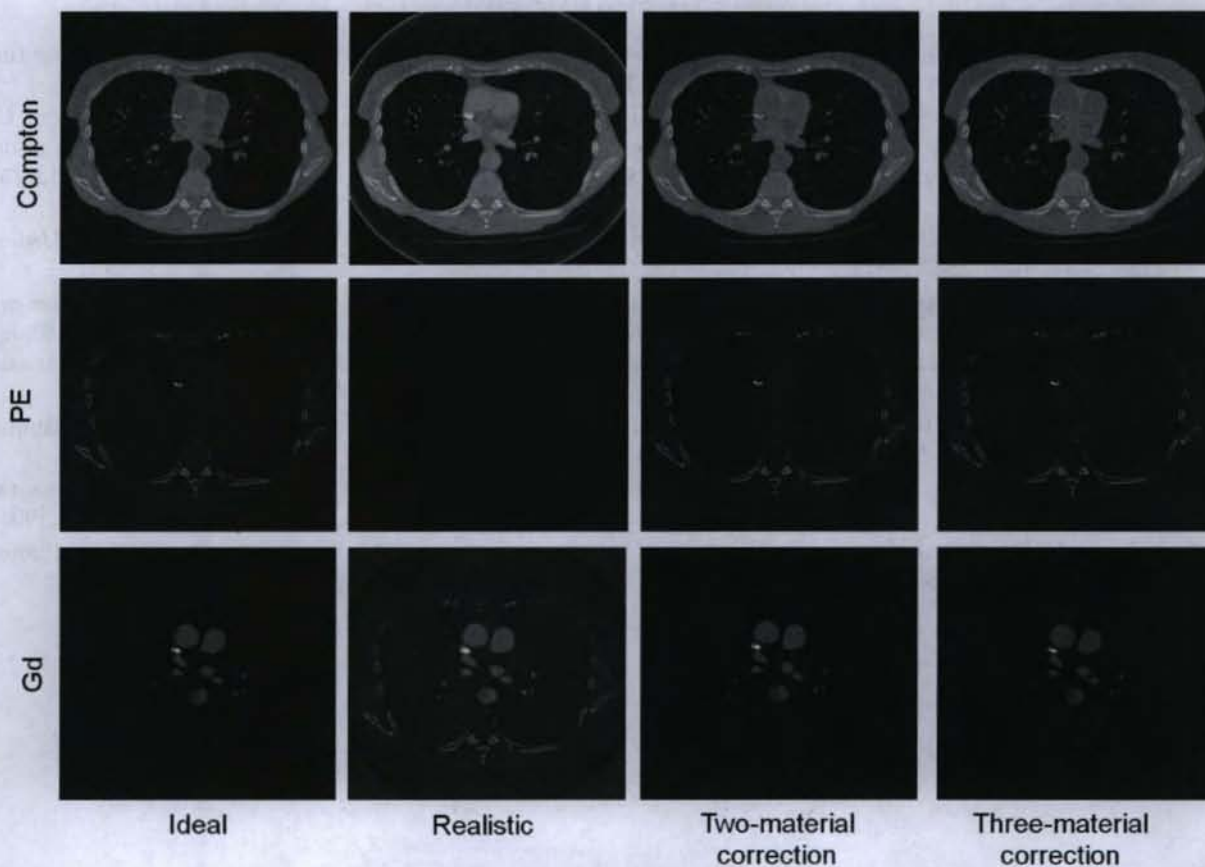


Figure 3. Reconstructed Compton, photoelectric, and gadolinium basis images reconstructed from a detector with an ideal response, realistic spectral response with and without the proposed two and three material correction.



three-material calibration provided increased accuracy compared to the two-material calibration in the presence of gadolinium. Additional improvements may be obtained by performing an iterative, simultaneous estimation of the incident spectrum and the spectral response. For some photons, the energy lost when a high-energy photon is detected in a low energy bin is transferred to neighboring pixels. Thus, additional improvement may be possible by incorporating a cross-pixel correction. In the three-material calibration simulated in this work, 30 transmission measurements were performed to estimate the 15 unknown values of the spectral-response matrix. Further work is required to optimize the number and thicknesses of materials used for calibration and to validate the performance of the method under experimental conditions. Overall, results suggest feasibility of an empirical spectral-response correction method that can be performed on the scanner.

## REFERENCES

- [1] Roessl, E. and Proksa, R., "K-edge imaging in x-ray computed tomography using multi-bin photon counting detectors," *Physics in Medicine and Biology* **52**(15), 4679–4696 (2007).
- [2] Schlomka, J. P., Roessl, E., Dorscheid, R., Dill, S., Martens, G., Istel, T., Bäumer, C., Herrmann, C., Steadman, R., Zeitler, G., Livne, A., and Proksa, R., "Experimental feasibility of multi-energy photon-counting K-edge imaging in pre-clinical computed tomography," *Physics in Medicine and Biology* **53**(15), 4031–4047 (2008).
- [3] Schmidt, T., "CT energy weighting in the presence of scatter and limited energy resolution," *Medical Physics* **37**, 1056–1067 (2010).
- [4] Ponchut, C., "Correction of the charge sharing in photon-counting pixel detector data," *Nuclear Instruments and Methods in Physics Research Section A: Accelerators, Spectrometers, Detectors and Associated Equipment* **591**(1), 311 – 313 (2008). Radiation Imaging Detectors 2007 - Proceedings of the 9th International Workshop on Radiation Imaging Detectors.
- [5] Cho, S., Sidky, E., Bian, J., and Pan, X., "Dual-energy technique at low tube voltages for small animal imaging\*," *Tsinghua Science & Technology* **15**(1), 79–86 (2010).
- [6] Cranley, K., Gilmore, B., Fogarty, G., and Desponds, L., "IPEM Report 78: catalogue of diagnostic x-ray spectra and other data," Tech. Rep. 78, The Institute of Physics and Engineering in Medicine (IPEM) (1997).
- [7] Berger, M., Hubbell, J., Seltzer, S., Chang, J., Coursey, J., Sukumar, R., and Zucker, D., "XCOM: Photon cross sections database," *NIST Standard Reference Database* **8**, 87–3597 (1998).